



Synthesis, Antibacterial, and Antifungal Activities of Hybrid Molecules Based on Alzheimer Disease Drugs and Bearing an Amino Acid Fragment [†]

Radoslav Chayrov ¹, Aleksandra Tencheva ¹, Hristina Sbirkova-Dimitrova ², Boris Shivachev ², Anna Kujumdzieva ³, Trayana Nedeva ³ and Ivanka Stankova ^{1,*}

¹ Department of Chemistry, South-West University “Neofit Rilski”, 66 Ivan Michailov str., 2700 Blagoevgrad, Bulgaria; rchayrov@swu.bg (R.C.); sany900@abv.bg (A.T.)

² Institute of Mineralogy and Crystallography “Acad. Ivan Kostov”, Bulgarian Academy of Science, 1113 Sofia, Bulgaria; sbirkova@mail.bg (H.S.-D.); blshivachev@gmail.com (B.S.)

³ Faculty of Biology, Sofia University “St. Kliment Ohridski”, 8 Dragan Tsankov str., 1164 Sofia, Bulgaria; kujumdzieva@biofac.uni-sofia.bg (A.K.); nedeva.ts@abv.bg (T.N.)

* Correspondence: ivastankova@abv.bg

[†] Presented at the 23rd International Electronic Conference on Synthetic Organic Chemistry, 15 November–15 December 2019; Available Online: <https://sciforum.net/conference/ecsoc-23>.

Published: 14 November 2019

Abstract: The objective of the current study was to develop novel compounds—memantine derivatives with antimicrobial activity designed for application in treatment of bacterial and fungal infections in patients suffering from Alzheimer’s disease. To realize this objective, a series of six memantine hybrid molecules were synthesized, characterized by ¹H NMR, ¹³C NMR, MS, X-ray, and tested for their biological properties as anti-Alzheimer agents and their antimicrobial potential.

Keywords: memantine; hybrid molecules; Alzheimer’s disease; antibacterial activity; antifungal activity; X-ray

1. Introduction

There have been links between Alzheimer’s disease (AD) and infections that cause a long-term activation of the immune system, a process known as chronic inflammation. Some of the infections that are thought to be linked to Alzheimer’s include herpes, pneumonia, and infection with bacteria [1]. In the last few decades, neonatal sepsis and meningitis (NSM) remain a leading cause of infant mortality and morbidity, despite the use and availability of antibiotics. Bacterial *E. coli* is the most common Gram-negative pathogen causing NSM [2]. Regardless of the remarkable successes, there is still an unmet need for new effective therapeutic approaches to treat the disease. On the other hand, chronic viral, bacterial, and fungal infections might be causative factors for the inflammatory pathway in AD [3]. However, it is not yet clear whether these infections might trigger Alzheimer’s or cause it to get worse. It could be that people with Alzheimer’s are more susceptible to picking up infections. The blood–brain barrier (BBB) protects the brain by controlling what substances can pass from the blood into brain tissue. In Alzheimer’s disease, the blood–brain barrier is damaged, particularly in the brain region affected by Alzheimer’s. Evidences suggest that inflammation, the Alzheimer’s hallmark amyloid protein and the ApoE4 gene, which are all linked to Alzheimer’s disease, can contribute to the breakdown of the blood–brain barrier. Once it has been weakened, bacteria, viruses, and other harmful substances can get through the BBB into the brain more easily. This may explain why certain viruses and bacteria, such as herpes and spirochetes, are more common in the brains of people with AD [4]. Using the blood–brain barrier (BBB) and RNA-sequence models, Nie, P. et al. undertook a drug repositioning study to identify unknown antimicrobial activities for

known drugs. The authors demonstrated for the first time that memantine (MEM), a drug approved by the Food and Drug Administration (FDA) for the treatment of Alzheimer's disease, can very effectively block *E. coli*-caused bacteremia and meningitis in a mouse model of NSM. MEM was able to synergistically improve the antibacterial activity of ampicillin in neonatal mice with bacteremia and meningitis and also significantly regulate anti-inflammatory factors.

In the present study, we report on the design, synthesis, and antimicrobial properties of new memantine derivatives functionalized with amino acids, e.g., peptidomimetics. The results of the study suggest that some of the memantine analogues reveal a potential for application as antimicrobial agents [5–10].

2. Materials and Methods

2.1. General

Unless otherwise stated, the starting materials, reagents, and solvents were obtained from commercial purchase and used as supplied without further purification. Analytical thin-layer chromatography (TLC) was run on Merck silica gel 60 F-254, with detection by UV light (254 nm). Memantine hydrochloride (MH) was purchased from Sigma-Aldrich (St. Louis, MO, USA), amino acids were purchased from Bachem (Berlin, Germany).

^1H and ^{13}C spectra were recorded on Bruker Avance II+ spectrometer (14.09 T magnet), operating at 600.11 MHz ^1H frequencies, equipped with a 5 mm BBO probe with z-gradient coil. The temperature was maintained at 293 K, using a Bruker B-VT 3000 temperature unit with airflow of 535 L/h. All chemical shifts are reported in parts per million (ppm), referenced against tetramethylsilane (TMS, 0.00 ppm) or using the residual solvent signal (7.27 ppm for CDCl_3 of 2.5 ppm for DMSO). Electrospray ionization–mass spectrometry (ESI–MS) experiments were acquired on Bruker Compact QTOF-MS (Bruker Daltonics, Bremen, Germany) and controlled by the Compass 1.9 Control software. The data analysis was performed and the mono-isotopic mass values were calculated using Data analysis software v 4.4 (Bruker Daltonics, Billerica, MA, USA). The analyses were conducted in the positive ion mode at a scan range from m/z 50 to 1000, and nitrogen was used as a nebulizer gas at a pressure of 4 psi and flow of 3 L/min for the dry gas. The capillary voltage and temperature were set at 4500 V and 220 °C, respectively. An external calibration for mass accuracy was carried out by using sodium formate calibration solution. The precursor ion of each compound was selected, and ESI–MS/MS analysis was performed by collision-induced dissociation (CID); nitrogen was the collision gas, and the collision energy varied from 5 to 40 eV. MSn experiments were conducted on an ion trap instrument Esquire 3000 (Bruker Daltonics, Bremen, Germany) and controlled by the Esquire Control 5.3.11 software. ESI–MS data were collected in positive-ion mode at a scan range from m/z 50 to 500. In all ESI–MS measurements, the nebulizer gas pressure was 124.1 kPa at a flow rate of 5 L min $^{-1}$; the desolvation temperature was 300 °C and capillary voltage was adjusted to 4000 V. The sample solutions were delivered to the nebulizer by a syringe pump (Cole Parmer, Vernon Hills, IL, USA) at a flow rate 3 $\mu\text{L min}^{-1}$.

2.2. Synthesis

General procedure: The compounds **1a–e** were synthesized with memantine according to a known procedure (Scheme 1). For the compounds **1a–e** (3 mmol), DIPEA (3.1 mmol) was added to a solution of TBTU (3 mmol) in CH_2Cl_2 (15 mL). After stirring, the mixture was treated with memantine (3 mmol), along with DMAP (3 mmol). This mixture was stirred at RT for 3 h, and then evaporated to dryness. The residues were purified by column chromatography using chloroform/methanol (95:5). The Boc-protected group was removed by TFA (5 mL) at 0 °C for 1 h. After that, TFA-AA-memantine derivatives were treated with ammonia solution.

Described compounds **3a–3d** were characterized recently by Stankova et al. (*Amino acids in press*).

Boc-Gly-Thz-memantine: ^1H (DMSO- d_6) δ (ppm): 0.84 (s, 6H, CH_3), 1.14 (m, 2H), 1.28 (d, 2H, $J = 12.2$ Hz), 1.36 (d, 2H, $J = 12.4$ Hz), 1.41 (s, 9H), 1.69 (m, 2H), 1.88 (m, 2H), 2.12 (m, 1H), 4.39 (d, 2H, $J =$

6 Hz), 7.25 (s, 1H, NH), 7.81 (t, $J = 6$ Hz, 1H), 8.06 (s, 1H). ^{13}C (DMSO- d_6) δ (ppm): 171.9 (CO-amide), 159.9 (CO-BOC), 156.2 (Cquat-Thz), 150.6 (Cquat-Thz), 123.6 (CH-Thz), 79.9 (Cquat), 53.1 (Cquat-BOC), 50.6 (CH₂), 47.4 (CH₂), 42.7 (CH₂), 42.4 (CH₂), 32.4 (Cquat), 30.5 (2 \times CH₃), 30.0 (CH), 28.6 (2 \times CH₃-BOC). Yield: 65%. ESI-MS: Molecular formula: C₂₂H₃₃N₃O₃S; M_{exact} : 419.59, M_{found} [M + H] 420.63.

Fmoc-Thz-Thz-Mem: ^1H (DMSO- d_6) δ (ppm): 0.84 (s, 6H, CH₃), 1.16 (m, 2H), 1.29 (d, 2H, $J = 12.2$ Hz), 1.37 (d, 2H, $J = 12.4$ Hz), 1.79 (m, d, 2H, $J = 11.6$ Hz), 1.68 (m, d, 2H, $J = 11.6$ Hz), 1.93 (m, 2H), 2.12 (m, 1H), 4.26 (t, 1H, $J = 6.5$ Hz), 4.42 (d, 2H, $J = 6.2$ Hz), 4.53 (d, 2H, $J = 6.7$ Hz), 7.34 (t, $J = 7.5$ Hz, 2H), 7.43 (t, $J = 7.5$ Hz, 2H), 7.45 (s, 1H), 7.72 (d, $J = 7.7$ Hz, 2H), 7.91 (d, $J = 7.7$ Hz, 2H), 8.20 (s, 1H), 8.35 (s, 1H). Yield: 65%. ESI-MS: Molecular formula: C₃₄H₃₄N₄O₃S₂; M_{exact} : 610.80, M_{found} [M + H] 611.76.

2.3. X-ray Crystallography

2.3.1. Sample Crystallization

In order to obtain single crystals with suitable quality, the dry powder substances of Beta-Alanine-Memantine (C₁₇H₂₇F₃N₂O₃) and 4-F-Phenylalanine-Memantine (C₂₃H₃₂F₄N₂O₄) were dissolved in ethanol, methanol, and acetone at room temperature. Large crystals (0.3 \times 0.2 \times 0.15 mm³) suitable for single crystal X-ray studies formed within 2–3 days by slow evaporation. Crystals were obtained from the three solvents used, but the best quality crystal grew in acetone conditions.

2.3.2. Data Collection and Crystal Structure Refinement

A single crystal was mounted on a glass capillary and all data were collected at room temperature (290 K) on an Oxford diffraction Supernova diffractometer using Mo-K α radiation ($\lambda = 0.71013$ Å) from micro-focus source. The determination of unit cell parameters, data integration, scaling and absorption corrections were carried out using the CrysAlisPro [11]. The phases were obtained by direct methods with ShelxS-2018. The refinement of the structure involved several cycles of refinement using full-matrix least-squares on F^2 with the ShelxL-2018 package [12]. The N hydrogen atoms were positioned from difference Fourier map, while all other hydrogen atoms were placed at idealized positions. The non-hydrogen atoms were refined anisotropically, and hydrogen atoms were refined using the riding model. Visual representation of the two molecules present in the asymmetric unit were carried out using ORTEP [13], while three-dimensional packing and hydrogen bonding interactions were drawn using Mercury [14]. The data in the Crystallographic Information File (coordinates, structure factors, etc.) were verified using IUCr checkCIF/PLATON [15].

2.3.3. Thermal Analyses

Differential thermal analysis (DTA) and thermo gravimetric measurements (TG) were carried out simultaneously in a thermal analyzer Stanton Redcroft STA780 under the following conditions: heating rate of 5 °C/min⁻¹, dry argon as a carrier gas (–30 mL/min⁻¹) and sample weight of 10–11 mg, in corundum crucible.

2.4. Biological Methods

Agar Disk-Diffusion Method

Agar disk-diffusion testing, developed in 1940 [16], is the official method used in many clinical microbiology laboratories for routine antimicrobial susceptibility testing. Nowadays, many accepted and approved standards are published by the Clinical and Laboratory Standards Institute (CLSI) for bacteria and yeasts testing [17]. In this well-known procedure, agar plates are inoculated with a standardized inoculum of the test microorganism. Then, filter paper discs (about 6 mm in diameter), containing the test compound at a desired concentration, are placed on the agar surface. The Petri dishes are incubated under suitable conditions. Generally, the antimicrobial agent diffuses into the

agar and inhibits germination and growth of the test microorganism, and then the diameters of inhibition growth zones are measured.

Standard Antibacterial in Vitro Metrics. Minimum inhibitory concentrations were investigated by Abedon [18].

Time-kill test for evaluation of bacteriostatic/bactericide activity [19].

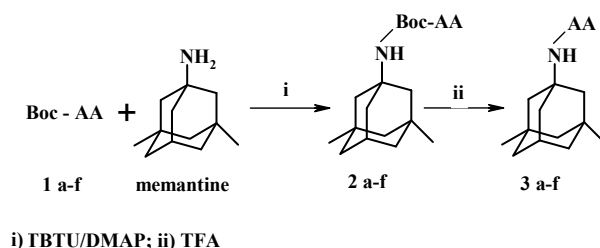
Test cultures were prepared as described above with an initial concentration of 0.1, 0.3, and 0.5 McF. To each culture was added 0.5 mL of 1 mM solution of test compound. Samples were incubated at 37 °C. OD₅₈₅ measurements were taken at 2, 3, 4, 5, and 6 h after incubation. In the samples, CFU/mL must be determined and compared to control data in same hour. The results are the following:

- if $x_i > x_k$ —the compound stimulates microorganisms to grow;
- if $x_i = x_k$ —the compound does not affect the microorganisms;
- if $x_i = \text{CFU/mL}$ before the incubation—the compound has a bacteriostatic effect;
- if $x_i < x_k$ —the compound has a bactericide effect.

3. Results and Discussion

Synthesis of novel compounds—memantine hybrid molecules, with antimicrobial activity, was designed for application in treatment of bacterial and fungal infections in patients suffering from dementia of Alzheimer's type.

The peptide bond between the memantine and amino acids and peptidomimetics was formed using the TBTU coupling reagent [20]. The protected groups were removed in CH₂Cl₂/TFA at 0 °C (Scheme 1).



Scheme 1. Synthesis of memantine derivatives substituted with amino acid and peptidomimetics **3a–f**, where: Glycyl-memantine (**3a**), 4-F-Phenylalanyl-memantine (**3b**), Valyl-memantine (**3c**), β -Alanyl-memantine (**3d**), Gly-Thiazolyl-memantine (**3e**), Gly-Thiazolyl-Thiazolyl (**3f**).

3.1. X-ray Study

Single crystal X-ray study showed that the compounds crystallize in a centrosymmetric manner (SG $P2_1/c$, No. 14) for the Beta-Alanine-Memantine and in a non-centrosymmetric manner (SG $P2_12_12_1$, No. 19) for the 4-F-Phenylalanine-Memantine. The asymmetric units of the two studied compounds are shown in Figures 1 and 2.

The bond lengths and angles of the two molecules are comparable (Tables 1 and 2). The aromatic ring system present in the 4-F-Phenylalanine-Memantine molecule is essentially planar with *rmsd* of 0.002 Å. The overlay of the two molecules shows that the memantine geometry is highly conserved.

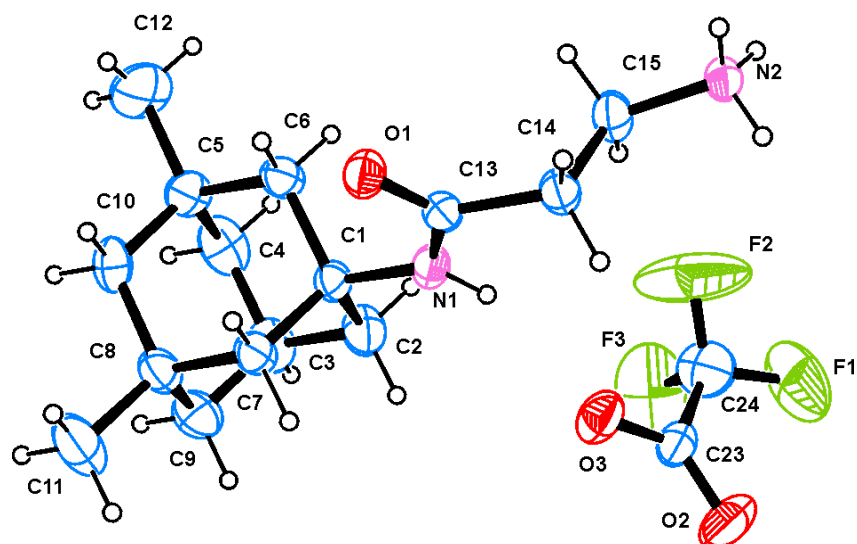


Figure 1. ORTEP [15] view of the β -Alanine-Memantine asymmetric unit along with atom numbering scheme. Atomic displacement parameters (ADP) are drawn at the 50% probability, while hydrogen atoms are shown as spheres with arbitrary radii.

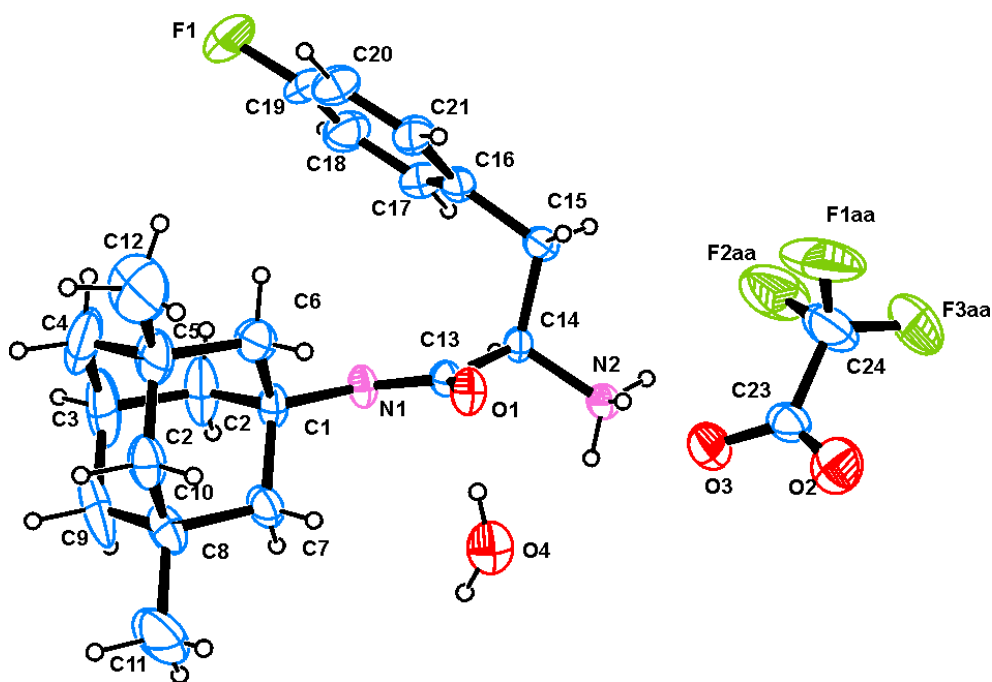


Figure 2. View of the 4-F-Phenylalanine-Memantine asymmetric unit and the applied numbering scheme. Atomic displacement parameters (ADP) are drawn at the 50% probability, while hydrogen atoms are shown as spheres with arbitrary radii.

Table 1. Selected geometric parameters for β -Alanine-Memantine and 4-F-Phenylalanine-Memantine. Bond Lengths [Å].

Bond	Length [Å] for β -Ala-Memantine	Length [Å] for 4-F-Phe-Memantine
O1–C13	1.219(5)	1.229(7)
N1–C1	1.485(5)	1.485(9)
N1–C13	1.336(6)	1.312(8)
C13–C14	1.513(6)	1.522(9)
C15–C14	1.478(6)	1.529(9)

C1–C7	1.523(6)	1.500(10)
C1–C2	1.523(7)	1.538(11)
C1–C6	1.516(6)	1.520(11)
C2–C3	1.534(7)	1.547(14)
C4–C3	1.517(9)	1.530(2)
C3–C9	1.502(9)	1.500(2)
C5–C4	1.524(8)	1.531(17)
C5–C12	1.529(8)	1.517(16)
C7–C8	1.538(6)	1.520(11)
C10–C8	1.527(7)	1.508(12)
C11–C8	1.539(8)	1.544(15)

Table 2. Selected geometric parameters for β -Ala-Memantine and 4-F-Phe-Memantine. Bond Angles/°.

Angle	Angle [°] for β -Ala-Memantine	Angle [°] for 4-F-Phe-Memantine
C13–N1–C1	126.6(4)	128.0(5)
O1–C13–N1	123.4(4)	126.3(6)
O1–C13–C14	120.8(4)	118.0(6)
N1–C13–C14	115.7(4)	115.6(5)
N1–C1–C7	110.3(4)	112.1(6)
N1–C1–C2	107.3(4)	104.7(6)
N1–C1–C6	110.8(4)	111.8(6)

The observed difference is related to the β -Alanine-Memantine and 4-F-Phenylalanine-Memantine orientation (Figure 3).

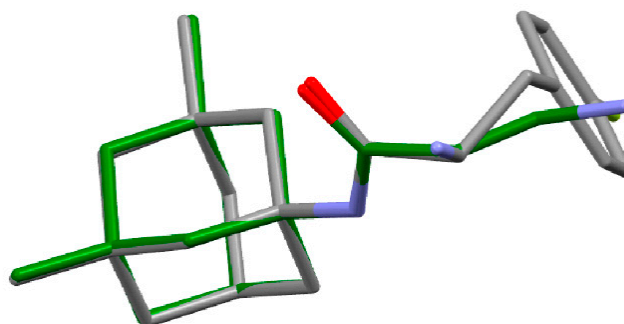


Figure 3. Overlay of the molecules of 4-F-Phenylalanine-Memantine and Beta-Alanine-Memantine based on the identical memantine moiety.

Having in mind the similarity (bond lengths and angles), one should expect similar hydrogen bonding interactions, as the side chain difference provides the main difference between the structures. Indeed, in both structures, intermolecular N–H \cdots O hydrogen bonds (Table 3) stabilize the three-dimensional packing of the molecules. The crystal structure of 4-F-Phenylalanine-Memantine and β -Alanine-Memantine also reveals the presence of Trifluoroacetic acid (TFA) that produces the zwitterionic structure. One solvent water molecule is present in the 4-F-Phenylalanine-Memantine.

Table 3. Hydrogen Bonds geometry (Å, °) (A) for β -Alanine-Memantine and (B) for 4-F-Phenilalanine-Memantine.

D-	H	A	d(D-H)/Å	d(H...A)/Å	d(D...A)/Å	D-H...A/°
N2-	H2A	O1 ¹	0.89	1.87	2.725(5)	161.1
N2-	H2B	O15 ²	0.89	1.92	2.725(5)	149.3
N2-	H2C	O4 ³	0.89	1.93	2.788(5)	162.3
N3-	H3	O4	0.86	2.12	2.908(5)	151.5
C6-	H6A	O1	0.97	2.61	3.169(6)	117
C8-	H8B	F2	0.97	2.56	3.467(9)	155.9
C14-	H14B	O1	0.97	2.45	3.047(6)	119.5
(A) β -Alanine-Memantine.						
D-	H	A	d(D-H)/Å	d(H...A)/Å	d(D...A)/Å	D-H...A/°
N2-	H2A	O11 ¹	0.89	2.15	2.916(9)	144.3
N2-	H2B	O8 ²	0.89	1.91	2.766(8)	161.2
N2-	H2C	O8	0.89	2.04	2.868(10)	153.9
N3-	H3	O4 ¹	0.86	2.1	2.942(8)	164.5
C7-	H7	O4 ¹	0.98	2.57	3.441(9)	147.3
C23-	H23B	O1	0.97	2.5	3.071(10)	117.8
(B) 4-F-Phenilalanine-Memantine.						

3.2. Thermal Behavior

The thermal behavior of the F-Phenilalanine-Memantine and β -Alanine-Memantine compounds was investigated between room temperature and 250 °C using DTA–TG–DTG analysis (Figure 4).

For the β -Alanine-Memantine (Figure 4A), DTA measurement shows a slow endothermic effect at 150–170 °C without loss of mass on the TG curve. Such kind of *endo* effect can be related to the melting point of the compound. A second *endo* effect is detected at higher temperatures of 200–250 °C. The second effect is accompanied by mass losses and can be associated with decomposition of β -Alanine-Memantine.

Similarly for the 4-F-Phenilalanine-Memantine (Figure 4B), DTA measurement shows two endothermic effects: the first is in the range 150–170 °C, and the second, 200–250 °C. The first *endo* effect is accompanied by ~3% weight losses, which corresponds to a loss of a water molecule and is in agreement with the crystal structure. The second DTA effect is associated with pronounced weight losses and is the melting and decomposition of the 4-F-Phenilalanine-Memantine. After the melting, a pronounced weight loss is started due to the volatility. The two processes—melting and decomposition—cannot be clearly separated, because they seem to occur almost simultaneously.

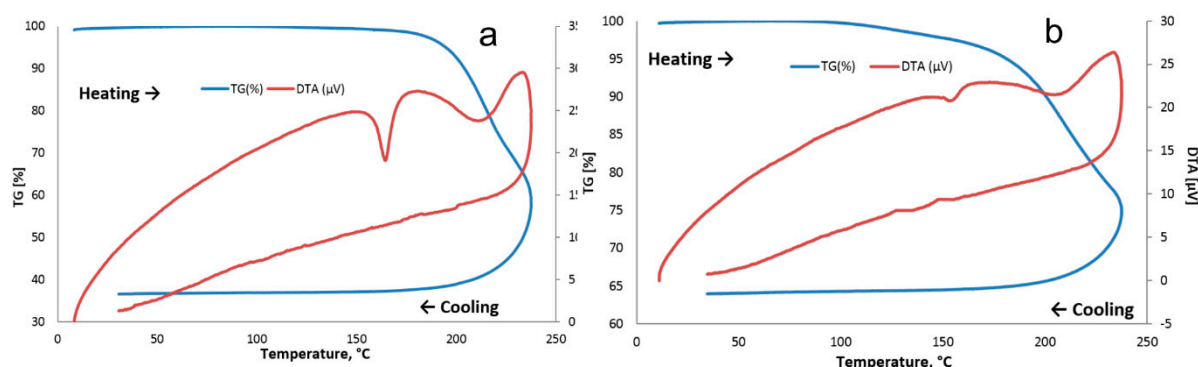


Figure 4. DTA–TG curves: β -Alanine-Memantine; 4-F-Phenilalanine-Memantine.

3.3. Biological Part

The new memantine analogues were investigated for antibacterial activity against model Gram-positive and Gram-negative bacteria and activity against yeast microorganisms—Gram-positive bacteria—*Staphylococcus aureus* NBIMCC (6538), *Bacillus megaterium*, Gram-negative bacteria—*Escherichia coli* (NBIMCC 3397), *Salmonella enterica* (NBIMCC 869) and yeasts—*Rhodotorula* sp. (BF 16-25), *Candida lusitanae* (BF 74-4). Antibacterial activity of investigated compounds are presented in Table 4. Two concentrations were prepared: 1 mM and 10 mM. The efficacy of the test compounds was determined by measuring the inhibition zone (in mm) and compared with the controls.

The compound 4-F-Phe memantine shows the highest antibacterial activity against both types of Gram bacteria. Its inhibition effect is similar with that of commercially available tetracycline (30 µg/disk). Antibacterial activity of compounds Val-memantine and Thz-memantine is lower and variable, between 10 and 16 mm inhibition area. Compound β-Ala-memantine demonstrates activity only against *S. enterica*, while compounds Gly-memantine and Fmoc-Thz-Thz-memantine are both inactive. All tested compounds were dissolved in DMSO. This solvent, 4-F-L-Phenylalanine, tetracycline, and the memantine (Nemdatine 10 mg tablets) were included as controls.

Comparing analysis of antimicrobial activity shows that compound Val-memantine has greater activity against Gram (−) bacteria. Among Gram (+) bacteria, only *Bacillus megaterium* growing was affected.

Table 4. Antibacterial activity of chemical derivatives of memantine (10 mM) against Gram (+) and Gram (−) bacteria. The area of inhibition are presented in mm.

Compound No. (10 mM)	Gram (−) Bacteria			Gram (+) Bacteria	
	<i>S. enterica</i>	<i>E. coli</i>	<i>St. aureus</i>	<i>B. megaterium</i>	<i>St. epidermidis</i>
Gly-memantine	n/a	n/a	n/a	n/a	n/a
4-F-Phe memantine	20	22	21	22	24
Val-memantine	11	11	n/a	16	n/a
β-Ala-memantine	16	n/a	n/a	n/a	n/a
Thz-memantine	n/a	13	10	16	n/a
Fmoc-Thz-Thz-memantine	n/a	n/a	n/a	n/a	n/a
Memantine.HCl	n/a	n/a	n/a	n/a	n/a
4-F-L-Phenylalanine	n/a	n/a	n/a	n/a	n/a
DMSO	n/a	n/a	n/a	n/a	n/a
Tetracycline	26	26	28	34	n/a

Compound β-Ala-memantine shows activity against *Salmonella enterica*, while Thz-memantine affects mostly Gram (+) bacteria with the exception of *Staphylococcus epidermidis*, which growing was not influenced. It is obvious that there is selectivity of inhibition among diverse memantine analogues. The exception is 4-F-Phe memantine, which affects the growing of all tested strains.

The investigation of 1 mM compounds concentration inhibitory effect was observed only at Gram (+) bacteria *St. aureus* and *B. megaterium* by compound 4-F-Phe memantine.

3.3.1. Yeasts

Yeasts are widespread in nature. Often they cause mycosis in individuals with immunocompromised status. The main causes are *Candida* and *Rhodotorula*. Recent studies indicate that the incidence of mycosis caused by *Rhodotorula* is between 0.5% and 20.3% in the US and Europe. The investigated isolates were resistant to the antibiotic fluconazole.

The antifungal activity data is presented in Table 5. The compound 4-F-Phe memantine 2 is the only one active against all tested yeast microorganisms. Its effect is similar to the well-known antifungal medication Nystatin. Compound Gly-memantine demonstrates activity only against *Sacch. cerevisiae*. Experimental data shows that the memantine derivatives have an antimicrobial effect against model prokaryote microorganisms and tested eukaryote cultures as well.

Table 5. Antifungal activity of chemical derivatives of memantine (10 mM) against model yeast microorganisms. The area of inhibition are presented in mm.

Compound № (10 mM)	<i>Rhodotorula sp.</i>	<i>Candida lusitaniae</i>	<i>Sacch. cerevisiae</i>
Gly-memantine	n/a	n/a	14
4-F-Phe-memantine	26	23	21
Val-memantine	n/a	n/a	n/a
β -Ala-memantine	n/a	n/a	n/a
Thz-memantine	n/a	n/a	n/a
Fmoc-Thz-Thz-memantine	n/a	n/a	n/a
Memantine.HCl	n/a	n/a	n/a
4-F-L-Phenylalanine	n/a	n/a	n/a
DMSO	n/a	n/a	n/a
Nystatin	26	24	n/a

3.3.2. Quantitative Analysis of Antimicrobial Activity: Determination of Minimum Inhibitory Concentration (MIC)

The results from the MIC test are presented in Table 6.

Table 6. Minimal inhibitory concentration values of memantine analogues.

Compound No. (μ M)	Gram (−) Bacteria		Gram (+) Bacteria		Yeasts	
	<i>S. enterica</i>	<i>E. coli</i>	<i>St. aureus</i>	<i>B. megaterium</i>	<i>Rhodotorula sp.</i> 16-25	<i>Candida lusitaniae</i> 74-4
Gly-mem (3a)	1.25	n/a	n/a	1.25	n/a	0.3125
4-F-Phe mem (3b)	0.156	1.25	1.25	0.625	0.078	0.078
Val-mem (3c)	1.25	5	10	2.5	n/a	0.3125
β -Ala-mem (3d)	n/a	10	n/a	n/a	n/a	0.078
Thz-mem (3e)	5	5	10	10	1.25	0.3125

Antibacterial activity against Gram (+) and Gram (−) bacteria could be evaluated by the following way:

- ✓ *E. Coli*—No. 3b > No. 3c, No. 3e;
- ✓ *S. enterica*— No. 3b > No. 3e > No. 3c;
- ✓ *St. aureus*— No. 3b > No. 3e > No. 3c;
- ✓ *B. megaterium*— No. 3b > No. 3c > No. 3e;
- ✓ *St. epidermidis*— No. 3b > No. 3c, No. 3e.

Compound Gly-memantine is active against *Salmonella enteria* and *B. megaterium* with MIC value 1.25 mM. Regarding β -Ala-memantine, we observed low antimicrobial activity (MIC = 10 mM) against *E. coli*. Compound 4-F-Phe-memantine demonstrated the highest antimicrobial potential against all tested microorganisms. The MIC values are in a wide range, from 1.25 mM to 0.078 mM. Compound Thz-memantine is also active against all tested microorganism at higher concentrations, compared to compound 4-F-Phe memantine. Val-memantine shows activity, but at high concentrations.

3.3.3. Time-Kill Test for Evaluation of Bacteriostatic/Bactericide Activity

Time-kill test of 4-F-Phe-memantine, conducted with the most sensitive bacterial species *Salmonella enterica*, shows bactericidal effect and 100% inhibition of bacterial growth after 7 h of cultivation in the presence of the test substance (Figure 5). For the same period, the control reached a cell density above 6×10^8 CFU/mL.

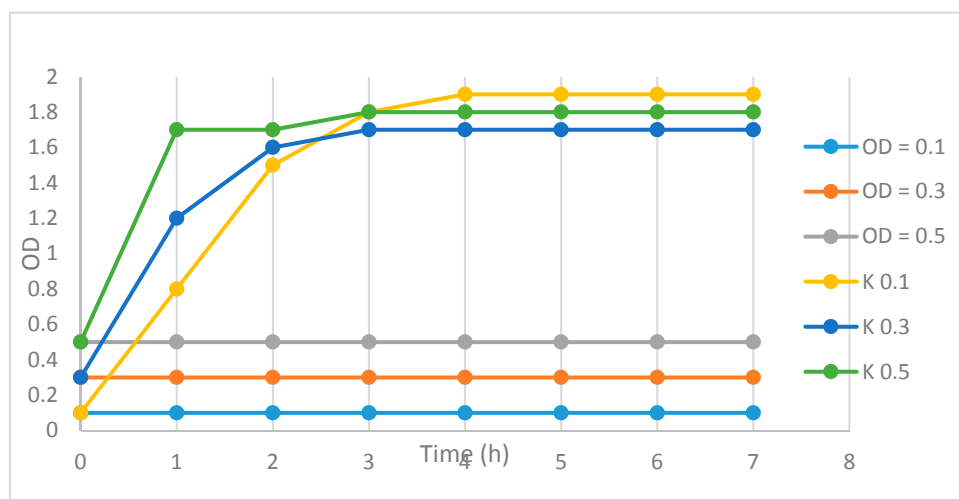


Figure 5. Dynamics of *Salmonella enterica* growth in the presence of 1 mM 4-F-Phe-memantine.

4-F-Phe-memantine showed a strong inhibitory effect on the growth of filamentous fungi (Table 7). It is in the range of 8% for *Penicillium chaviforme* and 62.9% for *Fusarium graminearum*.

Table 7. Inhibition of radial growth rate (Kr) of filamentous fungi in the presence of 4-F-Phe-memantine 3b.

Hours	<i>Penicillium chaviforme</i> d (mm)				<i>Fusarium graminearum</i> d (mm)			
	K	Topsin	DMSO	3b	K	Topsin	DMSO	3b
0	0	0	0	0	0	0	0	0
24	5, 6	0/0	9, 8	7, 6	10/7	15/16	20/22	7, 7
48	11, 12	0/0	14/13	11, 10	26/26	39/39	39/39	35/35
72	16/16	0/0	13/14	15/14	52/49	44/44	70/62	43/49
98	21/21	0/0	23/23	20/19	71/70	49/45	83/82	46/50
120	25/25	0/0	27/27	24/22	85/85	50/50	85/85	51/55
Kr (mm/h)	19, 7	0	17, 5	15, 7	84, 9	49, 8	84, 8	19, 8

4. Conclusions

The investigated memantine analogues with amino acids exhibit inhibitory effects on individual test microorganisms. Val-memantine shows greater efficacy against Gram-negative bacterial employees, and toward Gram-positive conditions that raise a plant only on the *Bacillus megaterium*. β -Ala-memantine has an effect exclusively on *Salmonella enterica* plants, and Gly-Thiazole has a good inhibitory effect against Gram-positive bacteria.

The 4-F-Phe-memantine was effective on all the strains required. The inhibitory effect is commensurate with this time to control the commercially available tetracycline and nystatin. The hybrid 4-F-Phe-memantine is the most promising for possible application as a new anti-infective host-directed therapeutic agent against clinically significant, conditionally pathogenic bacteria in patients suffering from moderate-to-severe dementia of Alzheimer's type.

Author Contributions: R.C.—synthesis and purification of compounds, A.T.—synthesis and purification of compounds, H.S.-D.—X-ray, B.S.—interpretation X-ray, A.V.K.—antimicrobial activity, T.N.—interpretation antimicrobial activity, I.S.—interpretation of structure/activity relationship. All authors have read and agreed to the published version of the manuscript.

Funding: We gratefully acknowledge the financial support from the Bulgarian Science Fund (Project M23/8) and South-West University Neofit Rilski (Project RPY-A3/19).

Conflicts of Interest: The authors declare no conflict of interest.

References

1. Aracava, Y.; Pereira, E.F.; Maelicke, A.; Albuquerque, E.X. Memantine blocks $\alpha 7$ nicotinic acetylcholine receptors more potently than n-methyl-D-aspartate receptors in rat hippocampal neurons. *J. Pharmacol. Exp. Ther.* **2005**, *312*, 1195–1205.
2. Nie, P.; Li, D.; Hu, L.; Jin, S.; Yu, Y.; Cai, Z.; Shen, L. Atorvastatin Improves Plaque Stability in ApoE-Knockout Mice by Regulating Chemokines and Chemokine Receptors. *PLoS ONE* **2014**, *9*, e97009.
3. Sochocka, M.; Zwolińska, K.; Leszek, J. The infectious etiology of Alzheimer's diseases. *J. Curr. Neuropharmacol.* **2017**, *15*, 996–1009.
4. The Infectious Etiology of Alzheimer's Disease, Alzheimer's Society Infections and Dementia. Available online: <https://www.alzheimers.org.uk/about-dementia/risk-factors-and-prevention/infections-and-dementia> (accessed on 25 October 2019).
5. Llor, C.; Bjerrum, L. Antimicrobial resistance: Risk associated with antibiotic overuse and initiatives to reduce the problem. *Ther. Adv. Drug Saf.* **2014**, *5*, 229–241.
6. Coates, A.R.M.; Novel, Y.H. Approaches to developing new antibiotics for bacterial infections. *Br. J. Pharmacol.* **2007**, *152*, 1147–1154.
7. Aminov, R. History of antimicrobial drug discovery: Major classes and health impact. *Biochem. Pharmacol.* **2017**, *133*, 4–19.
8. O'Neill, J. Antimicrobial Resistance: Tackling a crisis for the health and wealth of nations. *Rev. Antimicrob. Resist.* **2014**, *14*, 742–750.
9. Ibrahim, M.A.; Panda, S.S.; Birs, A.S.; Serrano, J.S.; Gonzalez, S.F.; Alamry, K.A.; Katritzky, A.R. Synthesis and antibacterial evaluation of amino acid-antibiotic conjugates. *Bioorg. Med. Chem. Lett.* **2014**, *24*, 1856–1861.
10. Powers, J.H. Antimicrobial drug development: The past, the present, and the future. *Clin. Microb. Infect. Dis.* **2004**, *10*, 23e31.
11. Crysalis PRO. Agilent Technologies; UK Ltd.: Yarnton, UK, 2011.
12. Sheldrick, G.M. A short history of SHELX. *Acta Cryst. A* **2008**, *64*, 112–122.
13. Sheldrick, G.M. Crystal structure refinement with SHELXL. *Acta Cryst. Sect. C* **2015**, *7*, 3–8.
14. McCoy, A.J.; Grosse-Kunstleve, R.W.; Adams, P.D.; Winn, M.D.; Storón, L.C.; Read, R.J. Phaser crystallographic software. *J. Appl. Crystall.* **2007**, *40*, 658–674.
15. Farrugia, L. WinGX and ORTEP for Windows: An update. *J. Appl. Cryst.* **2012**, *45*, 849–854.
16. Heatley, N.G. A method for the assay of penicillin. *Biochem. J.* **1944**, *38*, 61–63.
17. Balouiri, M.; Sadiki, M.; Ibnsouda, S.K. Methods for in vitro evaluating antimicrobial activity: A review. *J. Pharm. Anal.* **2016**, *6*, 71–79.
18. Abedon, S. Phage therapy pharmacology: Calculating phage dosing. In *Advances in Applied Microbiology*; Academic Press: Cambridge, MA, USA, 2011; Volume 77, pp. 1–40.
19. Payne, R.J.; Jansen, V.A. Understanding bacteriophage therapy as a density-dependent kinetic process. *J. Theor. Biol.* **2001**, *208*, 37–48.
20. Knorr, R.; Trzeciak, A.; Bannwarth, W.; Gillessen, D. New coupling reagents in peptide chemistry. *Tetrahedron Lett.* **1989**, *30*, 1927–1930.



© 2019 by the authors. Licensee MDPI, Basel, Switzerland. This article is an open access article distributed under the terms and conditions of the Creative Commons Attribution (CC BY) license (<http://creativecommons.org/licenses/by/4.0/>).